Near-threshold laser spectroscopy of iridium and platinum negative ions: Electron affinities and the threshold law

René C. Bilodeau, Michael Scheer,* and Harold K. Haugen†
Department of Physics and Astronomy, McMaster University, Hamilton, Ontario, Canada L8S 4M1

Robert L. Brooks
Department of Physics, University of Guelph, Guelph, Ontario, Canada N1G 2W1

(Received 14 July 1999; published 10 December 1999)

The electron affinity of Ir is measured to be 12617.4(12) cm^{-1} [1.56436(15) eV], from photodetachment studies on Ir^-. Previous measurements of the electron affinity of platinum reported results which were inconsistent within quoted error bars. A photodetachment study with a very improved energy resolution, signal-to-noise ratio, and signal-to-background ratio, was conducted on Pt^-, and yields a much more accurate electron affinity for Pt of 17140.1(4) cm^{-1} [2.12510(5) eV], in good agreement with the most recent measurement. Possible explanations for the poor agreement between the earlier results are discussed. In both the Ir^- and Pt^- spectra, the data indicate that the detachment cross section deviates from the expected Wigner threshold law, even near the detachment threshold. This behavior cannot be explained by the correction terms to the Wigner law proposed by the currently available threshold detachment models.

PACS number(s): 32.10.Hq, 32.80.Gc

I. INTRODUCTION

Over the past decades, many efforts have led to continually improved measurements of the bound states of atomic negative ions (for recent reviews on negative ions, see Refs. [1,2]). In addition to uses in a number of areas of pure and applied physics (such as ultrasensitive detection of atoms and isotopes in accelerator mass spectrometry [3]), negative ions have proven to be practical test subjects for subtle electron correlation and other quantum-mechanical effects. For example, negative ions have recently provided the means to enable the first direct observation of the radial component of an electronic wave function [4].

Two techniques are typically employed to study the bound states of atomic negative ions. In laser-photodetached electron spectrometry (LPES), fixed-wavelength laser light is used to photodetach the excess electron. The binding energy of the ion can then be deduced from the measured energy of the photoelectron. Although generally applicable to any atomic negative-ion system, LPES is limited by the resolution of the electron spectrometer. On the other hand, laser photodetachment threshold (LPT) spectroscopy uses a tunable light source to measure the threshold detachment energy. In this way LPT spectroscopy can achieve resolutions on the order of the bandwidth of the light source used and so very accurate measurements are possible, particularly when the excess electron is ejected into an *s*-wave continuum [5]. When an electron is ejected into a *p*-wave continuum, the very gradual onset of the photodetachment cross section near the threshold hampers the accurate determination of the threshold position. However, this technique has recently been successfully employed to obtain high accuracy measurements on the bound states of many *p*-wave detaching negative ions [6–8].

The present paper reports high resolution LPT measurements of Pt^- and Ir^-, from which high accuracy electron affinities (EA's) are deduced. The high-energy resolution and very low statistical noise obtained in these measurements have enabled the detection of a small, but clearly observable, deviation from the detachment cross-section behavior proposed by current threshold models. Similar deviations have previously been reported in negative ions for photon energies relatively far above the detachment threshold [9], but not for photon energies very near the threshold, as observed here.

II. EXPERIMENTAL METHOD

The apparatus is described in detail elsewhere [5], although for the present experiments no Raman conversion is required and hence none of the associated optical components are needed. Laser light of the required wavelength is produced using a dye laser pumped with the second harmonic of a Nd:YAG (yttrium aluminum garnet) laser, operating at a 10-Hz repetition rate. The laser beam is passed through a viewport into an UHV chamber to intersect with the negative ion beam at a 90° angle. The laser light is monitored with a pulse-energy meter located after the exit viewport to the vacuum chamber. Negative ions of the desired element are produced with a cesium sputter source. The ions are then accelerated, mass selected by 30° deflection in a magnetic field, charge state selected by electrostatic deflection plates, and sent into the UHV chamber. After crossing the laser beam, the residual ions are deflected by a second set of electrostatic plates and monitored in a Faraday cup, while the photodetached neutrals are detected with a discrete-dynode electron multiplier operating in an analog regime. The preamplified output signal is gated and integrated with a boxcar averager, and finally recorded with a personal computer for analysis.

*Present address: JILA, University of Colorado, Boulder, CO 80309-0440.

†Also with the Department of Engineering Physics, the Brockhouse Institute for Materials Research, and the Center for Electrophotonic Materials and Devices, McMaster University, Hamilton, Ontario, Canada.

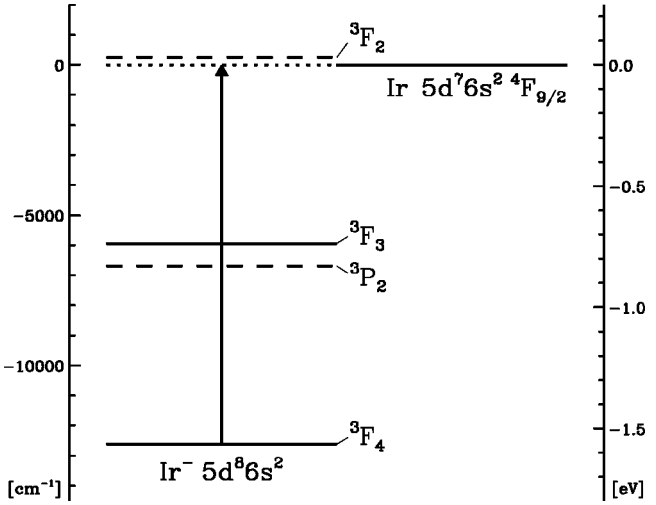

FIG. 1. Energy-level diagram for Ir^- and the ground state of Ir. Two of the negative-ion states have not yet been observed, and are located according to the predicted positions by long dashed lines in the figure. The vertical arrow indicates the detachment channel studied here.

The lasing wavelength is tuned so that the relative detachment cross section can be measured over a range of photon energies. The Wigner threshold law [10] predicts that the cross section is equal to 0 for photon energies smaller than the photodetachment threshold, and is proportional to $(\varepsilon-\varepsilon_0)^{l+1/2}$ for photon energies ϵ that are larger than the detachment threshold energy ε_0. The angular momentum l of the detached electron is 1 for the Ir^- and Pt^- ions studied here, resulting in a *p*-wave threshold. In practice, a small photodetachment background signal stemming from the detachment of excited negative ions and/or from ionic contaminants present in the ion beam is unavoidable, and must be fit to the observed spectrum (a more detailed discussion of the *p*-wave fitting procedure can be found in Ref. [6]). The cross section σ is then given by

$$\sigma=\begin{cases} a, & \text{for } \varepsilon\leqslant\varepsilon_0 \\ a+c(\varepsilon-\varepsilon_0)^{3/2}, & \text{for } \varepsilon>\varepsilon_0. \end{cases} \tag{1}$$

Here the constant a has been added to the Wigner law to account for a possible photodetachment background signal, and c is the proportionality constant implicit in the Wigner law. Additionally, a linear term may be included to account for a small slope in the background signal.

III. RESULTS

A. Ir^-

An energy-level diagram for the lowest-lying states of the Ir negative ion with respect to the ground state of neutral Ir is given in Fig. 1. The ionic states presented all have a $5d^86s^2$ configuration, the ground state being the $^3F_4$ level. On the basis of multiconfiguration Dirac-Fock calculations, the $^3F_3$ and $^3P_2$ states are predicted to be bound, while the $^3F_2$ state is expected to be slightly unbound [11]. Thøgersen *et al.* observed a $1+1$ photon detachment via a resonant magnetic dipole ($M1$) transition in Ir^-, locating the $^3F_3$ state at 7087.3(4) cm^{-1} above the ionic ground state [11]. The other two excited states have not yet been observed. There are two previous measurements of the binding energy of the $^3F_4$ level, and thus the EA of Ir. Using LPES, Feigerle *et al.* measured the EA of Ir to be 12630(65) cm^{-1} [12], and Davies *et al.* obtained an EA of 12613(4) cm^{-1} [13] using LPT spectroscopy.

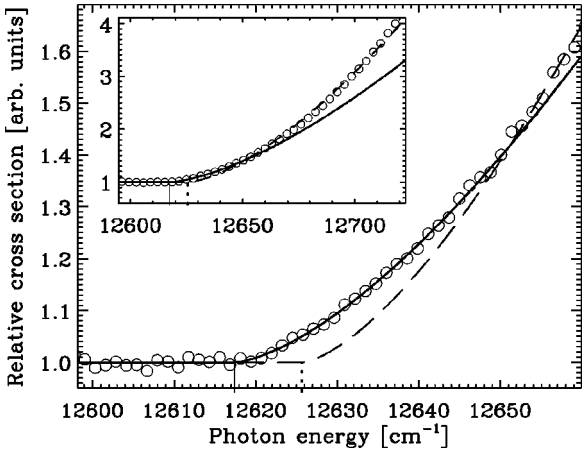

FIG. 2. Observed photodetachment spectrum of Ir^- near the ground-state detachment threshold, $^3F_4\rightarrow{}^4F_{9/2}$. The solid curve is the Wigner threshold law determined by the best fit to the data, including points below 12 650 cm^{-1} only. This is extrapolated to include the entire range of the inset. A solid vertical line marks the fitted threshold position. The dashed curve is a Wigner law fit to the entire scan range shown in the inset. On this scale the dashed line seems to agree quite well with the data, suggesting that this deviation could be easily overlooked in a lower-resolution scan. However, a poor fit is apparent near the threshold and a fitted threshold position (dashed vertical bar) significantly higher than the solid curve is obtained. See Sec. IV for further discussion on the observed deviation from the Wigner law.

A beam current of 100 nA of 8.5-keV Ir^- ions was obtained in the interaction chamber. A 120-cm^{-1} region including the $^3F_4\rightarrow{}^4F_{9/2}$ threshold was selected, and scanned five times in succession. No significant variation of the signal amplitude, threshold position, or threshold shape was observed in successive scans. The sum of the scans, normalized to the magnitude of the background signal, is presented in Fig. 2. From the fitted threshold one obtains the EA of Ir to be 12617.4(12) cm^{-1} [1.56436(15) eV, using 1 eV $=8065.5410\,cm^{-1}$ [14]] (all uncertainties, the sources of which are discussed in Sec. IV, are quoted to one standard deviation). This result is in good agreement with the previous measurements.

B. Pt^-

The accepted energy-level scheme for Pt^- is presented in Fig. 3. In addition to the $5d^96s^2\ ^2D_{5/2}$ ground state, two bound states are expected in Pt^-. The $^2D_{3/2}$ level has been measured via a bound-bound resonant $M1$ transition to lie 9740.9(5) cm^{-1} above the ionic ground state, while the $5d^{10}6s\ ^2S_{1/2}$ state is predicted to lie about 11300 cm^{-1} above

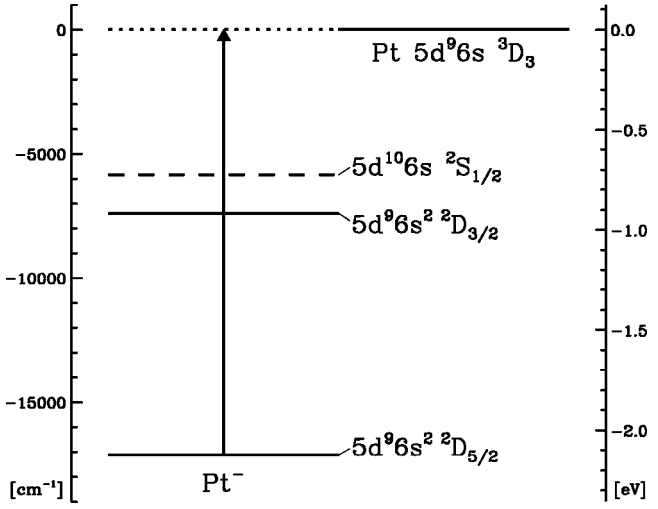

FIG. 3. Energy-level diagram for Pt^- and the ground state of Pt. The $^2S_{1/2}$ state has not been observed experimentally, and its expected position is indicated by a dashed line in the figure. The threshold studied in the present experiment is indicated by the vertical arrow.

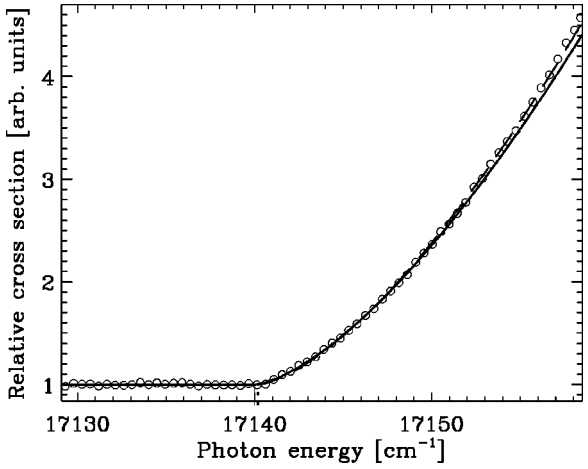

FIG. 4. The $^2D_{3/2}\rightarrow{}^3D_3$ detachment threshold in Pt^-. When only data points below 17150 cm^{-1} are included in the Wigner law fit, the solid curve is obtained. The dashed curve represents the Wigner law fit obtained when all the data points are included. As in Fig. 2, a small but conspicuous deviation from the Wigner threshold law is observed. The discrepancy is discussed in detail in Sec. IV.

the ground state on the basis of multiconfiguration Dirac-Fock calculations [11]. Three previous measurements of the EA of Pt have been performed. The photodetachment spectrum of a region including the $^2D_{3/2}\rightarrow{}^3D_3$ threshold was first measured by Hotop and Lineberger in 1973 [15], from which an EA of 17160(16) cm^{-1} was obtained. In 1992, Gibson *et al.* determined the EA of Pt to be 17125(9) cm^{-1} [16], which did not agree with the Hotop-Lineberger result within two standard deviations. Finally, a third measurement was reported in the 1996 paper by Thøgersen *et al.*, giving the EA of Pt as 17141(6) cm^{-1} [17], roughly equally spaced between the two previous results (see Sec. V for a summary of these results). Since all three experiments used the same ion production mechanism and experimental technique, the poor agreement between the three results is somewhat unexpected, and warrants further investigation. Therefore, we have measured the photodetachment spectrum of Pt^- near the ground-state detachment threshold with a set of very high-resolution scans.

A high-purity (99.98%) Pt metal pellet, set into an aluminum cathode mount, was used in the sputter source to produce 450 nA of 8.5-keV Pt^- ions in the interaction chamber. A much stronger detachment signal was observed for Pt^- than for Ir^-, mainly because an *s*-orbital electron is removed during photodetachment of Pt^-, while in Ir^- a *d* electron is removed, which is known to have a cross section typically about an order of magnitude smaller [12,18]. The larger ion current and laser-pulse energies available (30 mJ as opposed to 15 mJ for Ir^-) also increased the observed photodetachment signal. Because of the much stronger detachment signal, photon energies closer to the threshold could be scanned with the preservation of good statistics. The much smaller range (<30 cm^{-1}) scanned also reduces the uncertainty due to a possibly varying background signal, as was present in the Hotop-Lineberger experiment [15]. As with Ir, this range was repeatedly scanned, and only statistical variations in the spectrum were observed from one scan to the next. The sum of the scans, normalized to the below-threshold signal, is shown in Fig. 4. A threshold position of 17140.1(4) cm^{-1} [2.12510(5) eV] is obtained from the fit, a factor of 15 improvement in accuracy over the most recent result of 17141(6) cm^{-1} obtained by Thøgersen *et al.* [17]; the two results are in excellent agreement.

IV. DISCUSSION

The very slow onset of a *p*-wave threshold structure typically limits the accuracy with which the threshold position can be measured. However, the very good statistics obtained in the present experiments, especially for Pt^-, allow for an excellent fit to the data, and a careful consideration of potential systematic uncertainties is in order. These include uncertainties in the laser calibration, potential Doppler shifts, possible ponderomotive shifts, and uncertainties due to the Wigner approximation. A detailed discussion of the potential sources of errors associated with this apparatus can also be found elsewhere [5,6].

The dye laser tuning mechanism is calibrated against known optogalvanic lines obtained from a low-pressure Ar gas cell. A set of lines lying near the region of interest is measured immediately following each experiment, allowing for a calibration uncertainty of less than 0.2 cm^{-1} at the wavelengths used here. Small deviations from the nominally 90° angle between the laser beam and the ion beam in the interaction region can produce significant Doppler shifts. Therefore, care was taken to ensure that the angle could be realized to better than 1°, resulting in an uncertainty of less than 0.1 cm^{-1} for the photon energies and ion velocities in the present experiments. Very high-intensity light fields can also influence the apparent threshold position due to the ponderomotive potential [19]. However, for the relatively low intensities obtained in the interaction region a shift of $\ll 0.01$ cm^{-1} is expected, and is negligible in the present context.

Finally, the functional form of the fitting model itself must be considered. Due to the very gradual onset (zero slope) of the *p*-wave threshold, a sloped background signal can produce significant apparent shifts in the fitted threshold position. A small slope can be easily accounted for by including a linear term for the background in Eq. (1), fitted to a sufficiently large region below the detachment threshold and extrapolated above the threshold [6]. However, more insidious complications can come about due to nonlinear dependencies or fluctuations in the background signal, as are typically observed from the detachment of molecular ion impurities [20]. This can render the extraction of an accurate threshold value very difficult. Furthermore, such nonlinear fluctuations may be very difficult to detect if the photon-energy spacing and/or the statistical fluctuations of the data points are large. Therefore the Ir^- and Pt^- detachment thresholds of the present work were scanned with a very high-energy resolution (i.e., small spacing between data points), and with the very small statistical scatter that is seen in Figs. 2 and 4. The very small and flat signal observed below the threshold indicates that it is very unlikely that any energy-dependent structure due to impurities is present.

There is nonetheless a clear deviation from the expected Wigner threshold law in both the Ir^- and Pt^- detachment spectra presented here; in both cases the spectra above threshold appear to have a larger curvature than the 3/2 power law predicts. The dashed lines in Figs. 2 and 4 represent the fit to all the points in the data set. Only a very slight systematic deviation of the data from the dashed curve can be detected, demonstrating that such a subtle deviation could very easily be missed by a lower-energy-resolution scan. However, when only data very near the threshold are fit to the Wigner law, the deviation becomes very obvious (the solid curve in the figures). Furthermore, differences of 5 cm^{-1} (for Ir^-) and 0.2 cm^{-1} (for Pt^-) are observed in the threshold positions depending on whether the fit is made to all the data points or only to the data points near the threshold. Such a variation of the threshold position is not negligible. A second analysis of the Ag^- detachment spectrum previously measured by the authors [7] reveals the same effect is present in Ag (although it is far less conspicuous there, presumably because of the smaller energy range scanned in that experiment). Five main effects may be imagined to explain these observations: (1) a slowly (nonlinearly) varying background signal due to the detachment of some ionic impurity; (2) the onset of a second threshold or the presence of some broad continuum resonance structure located at slightly higher energies than the primary threshold; (3) the influence of some nonlinearity of the detection system; (4) the modification of the detachment cross section due to stray electric or magnetic fields; and (5) true deviations from the approximating threshold laws. These points are discussed in turn, listed (1)–(5) below:

(1) Mass-coincident, or nearly mass-coincident, weakly bound impurity negative ions present in the ion beam can produce a strong detachment signal. Furthermore, if the impurity is a molecular negative ion, as is commonly the case, then the presence of many closely spaced vibrational and rotational states can produce both sharp and slowly varying energy-dependent signals which can lead to a misinterpretation of the detachment spectrum. However, one would expect that the effects of such impurities would differ in different parts of the spectrum. Since the same increased curvature is observed in all three independent cases, with different masses and thresholds at differing photon energies, it would be an extremely unlikely coincidence for impurities to be responsible for the observed behavior.

(2) An increase in the detachment cross section associated with the onset of a second detachment channel can produce a structure similar to that observed here, as has been observed in a number of *p*-wave detaching species [6,8,15]. Fortunately the energy-level structure is relatively well known in all three cases [21], and no (observable) threshold is expected within many hundreds of wave numbers. Furthermore, assuming an effective ion source temperature of 1300 K, the excited-state populations in these ions would be $\sim 10^{-3}$ that of the ground state, and would thus produce a proportionally smaller detachment signal. It is therefore not possible to explain the observed threshold deviation on the basis of the onset of a second detachment channel.

(3) A nonlinear response of the detection system can be caused by changes in the amount of amplified spontaneous emission (ASE) present in the dye laser light, variations in the ion current, and nonlinear responses of the detector and/or amplification system. ASE of the laser is avoided by measuring the relative cross section in a very small region of the dye tuning range, over which the ASE component, if present, should not vary. Also, laser dyes are selected such that the scan range is near the maximum laser output, so as to minimize possible ASE components in the dye laser light. Furthermore, in the case of Pt and Ir experiments, the laser tuning curve was such that ASE would have been preferentially produced at photon energies below the detachment thresholds as the laser was tuned to larger photon energies. Therefore, a smaller detachment signal would be detected, contrary to what is observed here. The ion current was continuously monitored and no significant variations were observed. Performing multiple scans also helps to average random fluctuations in the ion-beam current. Saturation due to a signal level that exceeds the linear range of the detector or amplification system can also produce a nonlinear response of the detection system. Although only signals well within the design specifications of the electronics are measured, the linearity of the detection system was verified by monitoring the detachment signal obtained at a fixed wavelength, while varying the laser-pulse energy. Also, signal saturation results in a smaller detected signal, rather than the larger signal amplification that would be required to explain the deviations observed here. Finally, if a nonlinear response of any component of the detection system was present, one would also expect to have seen a similar effect in the high-resolution *s*-wave detachment spectra measured with this apparatus [5,22–26], but no such nonlinear response was noted.

(4) Static electric fields are known to have an observable effect on the photodetachment cross section of negative ions and have been thoroughly investigated in both *s*- and *p*-wave detaching species [27]. We have also observed this effect in C^- [5], Bi^- [25], and O^- [26] due to stray static electric

fields of 10–15 V/cm present in our system. In a *p*-wave detachment spectrum, such a stray electric field would produce an oscillation of the cross section with a period $\ll 10$ cm^{-1} and an amplitude of $\sim 10\%$, near the photodetachment threshold. Therefore, stray electric fields cannot explain the deviation observed here. Although similar periodic oscillations in the detachment cross section can be observed in a strong static magnetic field [28], the small field strengths expected in the interaction region (on the order of the Earth's magnetic field) would cause small oscillations with a period $\ll 0.001$ cm^{-1}, which does not produce any observable net effect. Finally, the oscillating electric and magnetic fields of the detaching laser light itself could change the structure of the detachment cross section. However, this effect would be limited to a range similar in magnitude to the ponderomotive potential ($\ll 0.01$ cm^{-1}, as discussed above) [19], and hence cannot account for the experimental observations.

(5) The Wigner threshold law describes the asymptotic behavior of the photodetachment cross section ''near'' the threshold [10]. The range of validity of the Wigner law is not predicted by the original work; however, two theoretical models have been developed to determine the magnitude and form of the leading corrections to the threshold law. The model developed by O'Malley [29] considered the effect of the polarizability α of the neutral atom [30] on the detachment cross section of negative ions, and predicted an increase in the cross section for *p*-wave detachment. Under this model the threshold law given in Eq. (1) should be modified to read, for $\varepsilon > \varepsilon_0$ (note that terms of order k^4 and higher in the square brackets [ ] have been dropped here),

$$\sigma = a + c(\varepsilon - \varepsilon_0)^{3/2}[1 - C_1 k^2 ln(a_0 k) + Dk^2], \qquad (2)$$

where a_0 is the Bohr radius, $C_1 = 4\alpha/15a_0$, D is a constant, and $k = \sqrt{2m_e(\varepsilon - \varepsilon_0)}/\hbar$ is the momentum of the detached electron, with m_e being the electron mass and $\hbar$ the Planck constant. The reader should note that the second term (the ''polarization term'') and the third term (the ''leading correction term'') in the square brackets [ ] have approximately the same dependence on k. Unfortunately, the theory does not predict the amplitude D of the leading correction term, and it is left as a fitting parameter. [O'Malley also considered the effects of a permanent electric quadrupole moment of the neutral. This correction was found to contribute with the same k dependence as the static polarizability but with a typically much smaller amplitude [29,31], and is not included in Eq. (2).] When Eq. (2) is fit to the Ir^- and Pt^- detachment data, the polarization term is found to account for less than 10% of the observed deviation from the Wigner law. One must therefore conclude that the polarization correction is insignificant compared to the leading correction term. This situation corresponds to the model developed by Farley [32], which has successfully described some photodetachment spectra (see, for example, Ref. [23]). Assuming that the polarizability of the atom is negligible ($\alpha = 0$), Farley used the zero-core-contribution approximation to obtain the constant D. However, the model predicts a reduction in the detachment cross section, contrary to what is observed here. Therefore, neither of the detachment models can fully characterize the spectra of the present work.

TABLE I. Comparison between current and previous electron affinity measurements.

Element	Measured EA[a] (cm^{-1})	$R = c/a$ (10^{-3} $cm^{3/2}$)[b]	Reference
Ir	12630(65)	N/A[c]	[12]
	12613(4)	5.5	[13]
	12617.4(12)	3.1	present work
Pt	17160(16)	0.12	[15]
	17125(9)	0.13	[16]
	17141(6)	1.1	[17]
	17140.1(4)	45	present work

[a]Uncertainties (appearing in parentheses) are quoted to one standard deviation.

[b]The constants c and a, respectively, are, the amplitude of the Wigner threshold law and the background level, as defined in Eq. (1). In these units, the numbers tabulated also correspond to the signal-to-background ratio 100 cm^{-1} above the detachment threshold (i.e., $[S_{100} - A]/A$, where S_{100} is the total signal observed 100 cm^{-1} above threshold, and A is the observed background signal).

[c]The Wigner threshold law is not applicable to the LPES measurement technique used in the experiment.

The source of the observed deviation from the Wigner threshold law is therefore not obvious. A number of other works have also found disagreements between observations and the available theoretical models, although at larger photon energies above threshold [9]. It therefore seems likely that an additional effect, beyond those considered in the current detachment models, is required in order to account for the observed deviation from the Wigner law. On the other hand, essentially identical threshold values are returned if any portion of the data is fit up to 35 cm^{-1} above threshold for Ir^- (or up to 10 cm^{-1} for Pt^-), suggesting that the Wigner law is valid up to that point, at least within the resolution of the data. The threshold values obtained from a fit to the Wigner law in these restricted regions are therefore used to obtain the quoted EA's. To accommodate the uncertainties in the fit (including the effect of a possibly sloped background) uncertainties of 1.2 and 0.3 cm^{-1}, for Ir and Pt, respectively, are assigned in addition to the possible systematic errors described above.

V. SUMMARY

A summary of the previous and present results is given in Table I. For ease of comparison, a graphical representation of the results is also provided in Fig. 5. The three Ir^- measurements are in good agreement. On the other hand, the Pt EA measurements agree less well. Although the large number of variables inherent in such experiments renders speculation difficult, some insight can be gained by comparing the spectra obtained in the four works.

As pointed out by Gibson *et al.* [16], the Hotop-Lineberger work [15] was primarily aimed at determining the range in which the Wigner law held, and therefore they

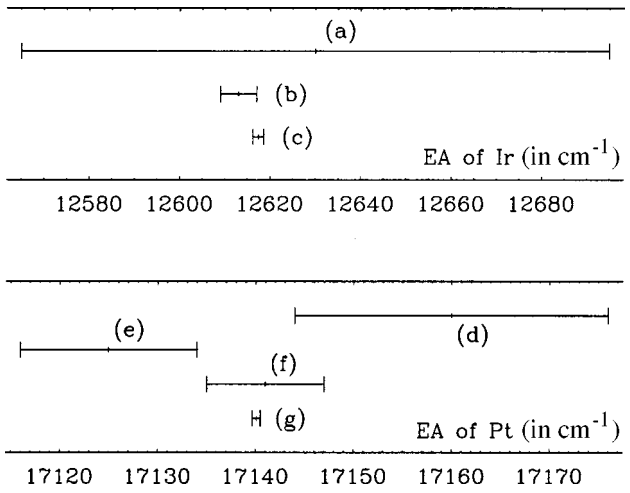

FIG. 5. Graphical representation of the previous (*a*, *b*, *d*, *e*, and *f*) and current (*c* and *g*) measurements of the electron affinities of Ir (top) and Pt (bottom). Note that the scales are different on the two sets. The results are, for Ir, (*a*) Feigerle *et al.* [12], (*b*) Davies *et al.* [13], and (*c*) present work. For Pt, (*d*) Hotop and Lineberger [15], (*e*) Gibson *et al.* [16], (*f*) Thøgersen *et al.* [17], and (*g*) present work.

acquired a spectrum over a large range of photon energies ($\approx$2000 cm^{-1}). A gradual change in the background signal was observed over this range, and had to be accounted for in the fit. To overcome this problem, Gibson *et al.* scanned only a 200-cm^{-1} range around the detachment threshold, and assumed a zero slope background, expecting that the background signal would be constant over this much smaller energy range. Finally, Thøgersen *et al.* scanned approximately the same range and obtained a third result that (marginally) agreed with the Hotop-Lineberger result, but did not agree with the value of Gibson *et al.* within error bars. In the present experiment, we scanned only a 30-cm^{-1} range, and obtained a value which agrees well with the result of Thøgersen *et al.*, but not with the previous two results. Although some of the discrepancy might be explained by an unnoticed deviation from the Wigner law, this is unlikely to explain the difference in the second and third results which cover essentially the same energy ranges. However, comparing the data plots of the four experiments suggests that the divergent results may also be due to the drastically different background levels observed in each experiment, perhaps stemming from molecular ion impurities. As previously noted, energy-dependent variations in the background signal can have a significant effect on the fitted threshold position [6,15,16].

The ratio $R=c/a$, with c the amplitude of the Wigner law fitting function and a the background level, as defined in Eq. (1), can be used as a measure of the signal-to-background ratio. The ratio R for each experiment is included in Table I for comparison (the values for the previous experiments can be easily deduced from the plots of the relative cross section found in the respective works). It can be noted from Table I that the (relative) background signal level changed by more than two orders of magnitude between the four experiments on Pt^-. Since all four experiments used the same type of ion production method (a sputter ion source), and since the fine-structure splitting of Pt^- is so large (nearly 10000 cm^{-1}), it is difficult to explain such a large difference in the observed background signals on the basis of varying amounts of excited-state populations in the ion beam. It is more likely that varying amounts of weakly bound ionic contaminants were present in the four experiments [20]. The much better signal-to-background ratio obtained in the current experiment (as indicated by the significantly larger ratio R) suggests that few or no impurities were present.

VI. CONCLUSIONS AND OUTLOOK

This paper has described high-precision measurements of the electron affinities of Pt and Ir, with significant improvements over previous results. Apparent disagreements in the previous EA measurements of Pt have been discussed, and are likely attributable to the much larger background signal observed in those measurements. A significant systematic deviation from the Wigner threshold law was observed in both detachment spectra, and remains unexplained under the currently available threshold models. This result strongly suggests that improvements in the threshold models may be necessary to obtain satisfactory fits to the increasingly higher-quality measurements now achievable with modern measurement techniques, even for photodetachment ranges restricted very near to the threshold. More advanced models would be particularly important for *p*-wave detaching elements because of the zero-slope onset of the threshold, which makes them especially sensitive to deviations from the threshold behavior. Further experimental work is also required to better understand the deviations observed here. Since the original work by Hotop and Lineberger [15], very few experiments have been aimed at explicitly establishing the range of validity of the threshold laws [31,33]. Considering the significant improvements to threshold measurement techniques in the past decades, a new comprehensive experimental study of this sort may now be appropriate. Good candidates for such studies on *p*-wave detaching species may be the precious metal and nickel group negative ions. In addition to the high sputter-ion currents easily obtainable for these elements, the threshold energies of these elements lie in easily accessible laser light regions, and therefore high-resolution data should be achievable. Furthermore, the relatively large energy spacings between the ionic states and between the low-lying neutral states in these elements reduce complications in the photodetachment spectrum over large energy regions. Exploring many ions with a similar electronic structure (such as all ions of a particular group) may also aid in identifying trends in the photodetachment behavior.

ACKNOWLEDGMENTS

Support for this work from the Natural Science and Engineering Research Council of Canada (NSERC) is gratefully acknowledged. We would also like to thank Victor Petrunin and Torkild Andersen for many interesting and helpful discussions.

[1] C. Blondel, Phys. Scr. **58**, 31 (1995); D. R. Bates, Adv. At. Mol. Opt. Phys. **27**, 1 (1991); T. Andersen, Phys. Scr. **34**, 23 (1991).
[2] T. Andersen, H. K. Haugen, and H. Hotop, J. Phys. Chem. Ref. Data (to be published).
[3] A. E. Litherland, Annu. Rev. Nucl. Part. Sci. **30**, 437 (1980); W. Kutschera and M. Paul, *ibid.* **40**, 411 (1990).
[4] C. Blondel, C. Delsart, and F. Dulieu, Phys. Rev. Lett. **77**, 3755 (1996).
[5] M. Scheer, R. C. Bilodeau, C. A. Brodie, and H. K. Haugen, Phys. Rev. A **58**, 2844 (1998).
[6] M. Scheer, C. A. Brodie, R. C. Bilodeau, and H. K. Haugen, Phys. Rev. A **58**, 2051 (1998).
[7] R. C. Bilodeau, M. Scheer and H. K. Haugen, J. Phys. B **31**, 3885 (1998).
[8] P. L. Norquist, D. R. Beck, R. C. Bilodeau, M. Scheer, R. A. Srawley, and H. K. Haugen, Phys. Rev. A **59**, 1896 (1999).
[9] Since models of the photodetachment threshold behavior are held to be true only ''near'' the detachment threshold, deviations from these predictions farther above the photodetachment threshold are not unexpected, and were observed in early photodetachment experiments (see Ref. [15] for example). However, it has proven very difficult to predict what photon energies are ''close enough'' to the threshold for the models to apply. For example, although the correction derived by Farley accurately described the photodetachment spectrum of B^- over a very large range [23], it was found to be inappropriate for the detachment spectrum of the very similar system Al^- [24,33].
[10] E. P. Wigner, Phys. Rev. **73**, 1002 (1948).
[11] J. Thøgersen, L. D. Steele, M. Scheer, H. K. Haugen, P. Kristensen, P. Balling, H. Stapelfelt, and T. Andersen, Phys. Rev. A **53**, 3023 (1996).
[12] C. S. Feigerle, R. R. Corderman, S. V. Bobashev, and W. C. Lineberger, J. Chem. Phys. **74**, 1580 (1981).
[13] B. J. Davies, C. W. Ingram, D. J. Larson, and U. Ljunblad, J. Chem. Phys. **106**, 5783 (1997).
[14] E. R. Cohen and B. N. Taylor, Rev. Mod. Phys. **59**, 1121 (1987).
[15] H. Hotop and W. C. Lineberger, J. Chem. Phys. **58**, 2379 (1973).
[16] N. D. Gibson, B. J. Davies, and D. J. Larson, J. Chem. Phys. **98**, 5104 (1993).
[17] J. Thøgersen, L. D. Steele, M. Scheer, C. A. Brodie, and H. K. Haugen, J. Phys. B **29**, 1323 (1996).
[18] P. C. Engelking and W. C. Lineberger, Phys. Rev. A **19**, 149 (1979); R. R. Corderman, P. C. Engelking, and W. C. Lineberger, J. Chem. Phys. **70**, 4474 (1979).
[19] R. Trainham, G. D. Fletcher, N. B. Mansour, and D. J. Larson, Phys. Rev. Lett. **59**, 2291 (1987); M. D. Davidson, J. Wals, H. G. Muller, and H. B. van Linden van den Heuvell, *ibid.* **71**, 2192 (1993).
[20] A number of molecular anions, with masses near that of Ir and Pt, are known to have photodetachment structure in the energy ranges of interest here. For example, signals from molecular impurities (attributed to the detachment of PtN^-) were studied by Hotop and Linberger [15]. An energy-dependent impurity signal was also observed during Davies *et al.* is photodetachment experiment on Ir^- (attributed to IrH^- at that time) [13]. We have observed similar detachment signals from an impurity molecule in this energy range (believed to be Cu_3^-). For more information on molecular negative ions, see for example, H. Hotop and W. C. Linberger, J. Phys. Chem. Ref. Data **4**, 539 (1975).
[21] *Atomic Energy Levels*, edited by C. E. Moore, Natl. Stand. Ref. Data Ser.–Natl. Bur. Stand. (U.S.) (U.S. GPO, Washington, DC, 1971), Vol. III.
[22] M. Scheer, R. C. Bilodeau, and H. K. Haugen, J. Phys. B **31**, L11 (1998); M. Scheer, H. K. Haugen, and D. R. Beck, Phys. Rev. Lett. **79**, 4104 (1997).
[23] M. Scheer, R. C. Bilodeau, and H. K. Haugen, Phys. Rev. Lett. **80**, 2562 (1998).
[24] M. Scheer, R. C. Bilodeau, J. Thøgersen, and H. K. Haugen, Phys. Rev. A **57**, R1493 (1998).
[25] R. C. Bilodeau, M. Scheer, and H. K. Haugen (unpublished).
[26] M. Scheer, Ph.D. thesis, McMaster University, 1998.
[27] N. D. Gibson, B. J. Davies, and D. J. Larson, Phys. Rev. A **47**, 1946 (1993); **48**, 310 (1993) (and references therein).
[28] O. H. Crawford, Phys. Rev. A **37**, 2432 (1988); D. J. Larson and R. Stoneman, *ibid.* **31**, 2210 (1985); W. A. M. Blumberg, W. M. Itano, and D. J. Larson, Phys. Rev. A **19**, 139 (1979).
[29] T. F. O'Malley, Phys. Rev. A **137**, A1668 (1965). Note: the polarization term appeared with the incorrect sign here (see, for example, Ref. [15]). The correct sign is used in Eq. (2).
[30] Approximate (calculated) ground-state static polarizabilities of 50, 51, and 44 atomic units for Ag, Ir, and Pt, respectively, can be found in complied tables. See, for example, V. P. Shevelko, in *Atoms and Their Spectroscopic Properties*, edited by G. Ecker, P. Lambropoulos, I. I. Sobel'man, H. Walther, and H. K. V. Lotsch (Springer, New York, 1997).
[31] R. D. Mead, Keith R. Lykke, and W. C. Lineberger, in *Photodetachment Threshold Laws*, Invited Papers of the XIII International Conference on the Physics of Electronic and Atomic Collisions, Berlin, 1983, edited by J. Eichler, I. V. Hertel, and N. Stolterfoht (Elsevier, New York, 1984).
[32] J. W. Farley, Phys. Rev. A **40**, 6286 (1989).
[33] D. Calabrese, A. M. Covington, J. S. Thompson, R. W. Marawar, and J. W. Farley, Phys. Rev. A **54**, 2797 (1996).